Phosphorus internal loading and sediment diagenesis in a large eutrophic lake (Lake Chaohu, China)[☆]

Chunhui Yang [a,b], Jiying Li [c], Hongbin Yin [a,*]

[a] State Key Laboratory of Lake Science and Environment, Nanjing Institute of Geography and Limnology, Chinese Academy of Sciences, 73 East Beijing Road, Nanjing, 210008, PR China
[b] University of Chinese Academy of Sciences, 19 Yuquan Road, Beijing, 100049, PR China
[c] Department of Ocean Science and Hong Kong Branch of Southern Marine Science and Engineering Guangdong Laboratory (Guangzhou), Hong Kong University of Science and Technology, Clear Water Bay, Hong Kong, People's Republic of China

ARTICLE INFO

ABSTRACT

Sediment phosphorus (P) release and retention are important in controlling whole-system P dynamics and budget in eutrophic lakes. Here we combine short- (seasonal) and long-term (years to decades) studies to quantify the internal P loading and P release potential in the sediments of Lake Chaohu and explore their controlling mechanisms. In the west region of the lake, short-term P diffusive fluxes ranged from 0.2 mg/m^2·d^{-1} to 6.69 mg/m^2·d^{-1} (averaged 2.76 mg/m^2·d^{-1}) and long-term net P release ranged from 2.25 mg/m^2·d^{-1} to 8.94 mg/m^2·d^{-1} (averaged 5.34 mg/m^2·d^{-1}); in the east region, short-term P diffusive fluxes varied from 0.73 mg/m^2·d^{-1} to 1.76 mg/m^2·d^{-1} (averaged 1.05 mg/m^2·d^{-1}) and long-term P release ranged from 0.13 mg/m^2·d^{-1} to 4.15 mg/m^2·d^{-1} (averaged 1.3 mg/m^2·d^{-1}). Both short- and long-term P releases were in the same order of magnitudes as the external P inputs (3.56 mg/m^2·d^{-1}). Comparison of the long-term and short-term sediment P release indicates that while the high summer P release in the east might only represent a snapshot value, the sediments in the west contribute to large P release for years or even decades, impeding water quality recovery under lake management. Mobilization of surface sediment legacy P accounted for 81% of short-term P release. The long-term release was dominated by remobilization of iron bond P (BD-P) (average 52.1%) at all sites, while Aluminium-bound P (NaOH-rP) exhibited partly reactive and potentially mobile, releasing P to the water column in most sites in the west. Our study demonstrates the importance of sediments as P sources in lake Chaohu. The combination of short- and long-term P release studies can help understand the roles of sediments in regulating the water quality and eutrophication.

1. Introduction

Phosphorus (P) is an essential macronutrient supporting primary productivity and is one of the possible limiting elements that can induce lake eutrophication (Schindler et al., 2016). Even when external P loadings are under control, the high concentrations of P accumulated in sediment, often termed as "legacy P″, can be released into the water column for many decades, delaying the recovery of the ecosystems (Sondergaard et al., 2003). It is important to quantify sediment P retention and release and understand how they responds to changing conditions, as they help to guide lake restoration management practices.

Phosphorus fluxes across the sediment-water interface (SWI) are driven by processes including the degradation of organic debris and the dissolution of iron oxyhydroxide close to the SWI. Both processes can increase P concentrations in the overlying waters and induce extensive algal bloom and other water quality problems, especially in the summer (Ingall and Jahnke, 1994, Katsev S. et al., 2006, Matisoff and Carson, 2014, Ribeiro et al., 2008). Phosphorus fluxes across SWI are often quantified using Fick's first law, a common method to quantify sediment P release (Ding et al., 2018; Dittrich et al., 2013; Matisoff et al., 2016; Tammeorg et al., 2015; Zhang et al., 2006). However, this estimate only quantifies the short-term P release through transient processes, on daily and/or seasonal time scales (Dittrich et al., 2013; Hupfer and Lewandowski, 2008; Markovic et al., 2019). In shallow eutrophic lakes, P released from sediment processes may redistribute among different P binding pools and accumulate as sediment legacy P, which can be

---

released over the long term (Parsons et al., 2017).

The long-term P release can be determined considering the mass balance among P supply, binding, and burial on scales of years to decades, which are controlled by sediment mineralogical composition and diagenetic processes (Depew et al., 2018; Dittrich et al., 2013; Kim et al., 2013; Matisoff et al., 2016; Ozersky et al., 2013). During sediment diagenesis, while some labile (reactive) P forms can be released to dissolved bioavailable forms, some labile P can also transfer into inert P forms that can be permanently buried (Alam et al., 2020; Dittrich et al., 2013). The rates of sediment burial and the sediment P content can be used to quantify the long term P retention, and its decrease with depth represents the potential long-term P release of the P pools (Dittrich et al., 2013; Hupfer M. and Lewandowski 2005; Rydin et al., 2011). While short-term P releases calculated from the dissolved concentration gradients at the SWI reflect the transient fluxes, the long-term sediment P retention and release calculated from the solid P forms regulate the ecosystem health for years and decades. Short-term fluxes need to be estimated to understand the role of sediment on short-term processes such as summer algal bloom, and long-term fluxes predict P dynamics over the long term.

Quantifiying the sediment P speciation and their vertical distributions helps to understand their potential mobility and contributions to long-term P release. By looking at the variations in the solid P phases, one can distinguish the long-term buried P and the P temporarily stocked in sediment (e.g., during seasonal variations in dissolved oxygen, pH, redox conditions), which can be released and/or redistributed. It also helps evaluate the potential mobilization of various P fractions that are considered inert. For example, apatite (HCl–P) and aluminum-bound P (NaOH-rP) are often regarded as inert and can be buried in sediment over a long time (Carey and Rydin, 2011; Malmaeus et al., 2012; Matisoff et al., 2016), but they can become mobile under certain environmental conditions (such as high pH) as suggested by many studies (Lukkari et al., 2007; Markovic et al., 2019; Yang et al., 2020).

Lake Chaohu is a typical large shallow lake in China that has been suffering from severe eutrophication and algal blooms for decades. Researchers have made efforts to understand the internal P loading in Lake Chaohu in recent years. Internal loading in surface sediments and diffusive fluxes have been determined at a few locations in the west of the lake (Yang et al., 2020). Sediment P geochemistry showed that the distribution of organic P fractions and their relative contribution to total P exhibited strong spatial variability responding to exogenous pollution input (Zan et al., 2011). However, lake-wide internal phosphorus loading from sediments and its contributions to lake-wide P cycling remain poorly constrained. Here, we (1) investigate the sediment P speciation, their vertical distributions and spatial variability in Lake Chaohu, (2) quantify the sediment mobile P pools and estimate the short-term and long-term P release and retention, and (3) investigate the roles of sediment P release to the lake-wide P cycle and how sediment P release respond to and affect water quality management.

2. Materials and method

2.1. Site description

Lake Chaohu is the fifth largest freshwater lake in China (117°16′54″-117°51′46″E, 31°25′28″-31°43′28″N), with a surface area of 768 km^2 and a mean depth of 2.7 m (Fig. 1). The Laoshan Island (117°25′50.84″-117°26′45.11″E, 31°33′41.43″- 31°34′10.15″N) divides the lake into two regions, the west (S1, S2, S3, S4, S5; area 250 km^2) and the east (S6, S7, S8, S9, S10, S11, S12; area 518 km^2). The lake has ten main tributaries (Fig. 1), of which Yuxi River was the only outflow river that exchanges water between Lake Chaohu and the Yangtze River. Five other major inflowing rivers (Nanfei, Pai, Hangbu, Baishitian, and Zhegao Rivers), account for more than 90% of runoff in the Chaohu basin (Tu et al., 1990). The lake played an important role in flood control, water supply, irrigation, transportation, fishery and tourism
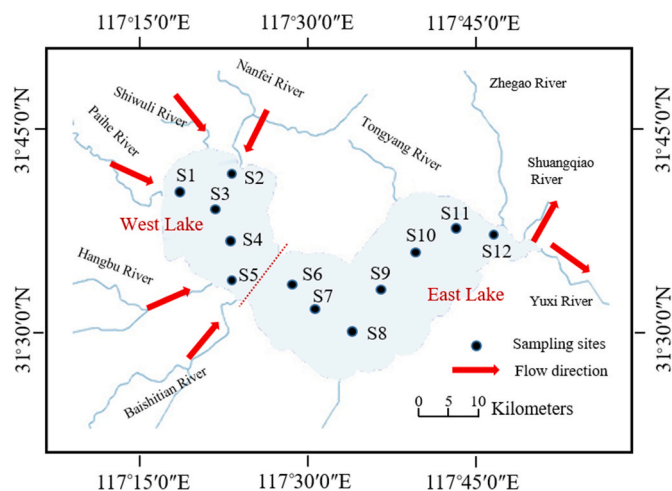

Fig. 1. Map of sampling sites in Lake Chaohu.

before the 1960s. Since 1995, with the rapid economic growth, agricultural runoff and industrial wastewater have seriously contaminated the inflowing rivers. The severe eutrophication and harmful algal bloom then have been a major and consisting environmental problem in Lake Chaohu, although pollution treatment projects of more than 20 years have been conducted to improve the water quality (e.g., sewage emission reduction and ecological restoration).

2.2. Water and sediment sampling,handling and chemical analyze

The samples were collected in July 2019 (location shown in Fig. 1). Surface water samples of 500 mL were collected into pre-cleaned polyethylene bottles and brought back to the laboratory to analyze for soluble reactive phosphorus (SRP), total phosphorous (TP) and chlorophyll-a (Chl-a) as quickly as possible. The concentrations of SRP were determined using molybdenum blue methods (Murphy and Riley, 1962). Total phosphorus were extracted using alkaline potassium persulfate followed by analysis of SRP concentrations in the extracts using a UV-2550 spectrophotometer (Chinese EPA, 2002). The concentration of Chlorophyll-a (Chl-a) was measured using acetone method with a fluorescence spectrophotometer (RF-5301PC) (Ritchie, 2006). Three sediment cores per site were collected using an 85-mm diameter, 600-mm-long core sampler (Rigo Co., Ltd., Tokyo, Japan) and transported to the laboratory within 3h after the collection without disturbing the SWI. These sediment cores were then incubated in a thermostatic circulator bath in the laboratory to deploy a high-resolution Peepers (HR-Peeper), by slowing inserting the HR-Peepers into the sediments to incubate for 24h under the same temperature as the in-situ water to reach equilibrium for measurement of porewater chemistry. (Ding et al., 2018). After incubation, the HR-Peepers were slowly and vertically removed from sediments to avoid the destruction of the sediment integrity. The porewaters obtained from HR-peepers were analyzed for concentrations of PO_4^{3-}, Fe^{2+}, NH_4^+ and the diffusive fluxes of the measured speciese were calculated (methods for chemical analyses of the porewaters and calculations of diffusive fluxes are shown in the supplementary material). The sediments after peeper retrieval were sliced vertically with increasing depth-intervals (at 2-cm intervals close to the SWI, at 3-cm intervals after 2 cm, at 5-cm intervals after 5 cm, and at 10-cm intervals after 10 cm) for analyses of porosity, organic matter, total nitrogen (TN), P binding forms, and total P (TP) (sum of six P binding forms). Organic matter was measured using potassium dichromate oxidation followed by heating with an oil bath (Qian et al., 2011). TN in sediment was extracted using alkaline potassium persulfate and then analyzed with a UV-VIS spectrophotometer (Chinese EPA, 2002). The sediments were oven-dried and sequentially extracted into six P

fractions (labile P (NH_4Cl–P), redox-sensitive P (BD-P), aluminum-bound P (NaOH-rP), the organic P (NaOH-nrP), other inorganic P (HCl–P) and residual P (Res-P)). Detailed sequential extraction methods are shown in the supplementary material.

2.3. Statistic analyses

Data were all ploted using Origin 8.5 software (OriginLab, Northampton, MA, USA). The IBM SPSS Statistics, ver. 19.0 (IBM, New York, NY, USA) was used to analyze the significant differences among parameters with one-way analysis of variance (ANOVA) followed by Duncan's test; The significance of the differences was reported at $p < 0.05$ and $p < 0.01$.

2.4. Potential mobile P pool

We estimate the potential mobile P pools using a mass balance approach. Sediment P content commonly shows the highest P concentrations in the surface layers that decrease with depth (Carey and Rydin, 2011; Markovic et al., 2019). The depth below which the P content no longer decreases represents the stabilization depth of P, below which P can be assumed to be permanently buried (Markovic et al., 2019) and the average P concentrations there can be regarded as burial P concentrations. Assuming steady-state accumulation, in the sediments above the stabilization layer, the P concentrations that exceed the burial P concentration can be assumed to be mobile, and its integral along the whole sediment column represent the potential capacity of long-term sediment P mobilization (Carey and Rydin, 2011; Markovic et al., 2019; Puttonen et al., 2014; Rydin, 2000; Rydin et al., 2011), which can be calculated as (Markovic et al.,(2019):

$$P_{mobile}(g \, / \, m^2) = \sum_{i=1}^{n} \Delta c_i \rho_i x_i$$

where Δc_i (g/kg) represents the differences between P binding forms at stabilization depth and each layer i above it; ρ_i (kg/m³) represents dry bulk density, and x_i (m) represents the thickness of each layer. We used this formula to the calculate P release of all P fractions and the sum of them to quantify the contribution of each P form to the total P release.

2.5. Sedimentation rates and long-term P release

Sediment cores were sampled at different locations in Lake Chaohu for dating (33–76 years from surface to deepest sediments in this study) and estimating sedimentation rates. Sediments were sliced into 2 cm intervals for analyses of ^{210}Pb activity using a high purity germanium well-type detector (HPGe GWL-120-15; EG & G Ortec, USA) at the State Key Laboratory of Lakes and Environment, Nanjing Institute of Geography and Limnology, Chinese Academy of Sciences. The sediment ages and mass accumulation rates were calculated using the accumulated excess ^{210}Pb activity and dry bulk density with the constant rate of supply (CRS) model. The detailed method can be found in the Supplementary Material. Assuming steady-state P sedimentation, the long-term P release can be calculated as the difference between P accumulation at the sediment surface and P burial at its stabilization depth (Markovic et al., 2019):

$$P_{release}(g \, / \, m^2 \cdot y^{-1}) = C_0 \times U_0 - C_s \times U_s$$

where C_0 (mg/g) and U_0 (g/m²·y⁻¹) represent dry sediment P concentration and dry sedimentation (accumulation) rate in the top layer, respectively, while C_s and U_s represent the P concentration and sedimentation (burial) rate at the stabilized layer, respectively (Alam et al., 2020; Markovic et al., 2019). For better comparasin between short- and long-term P release, the unit were unified into "mg/m²·d⁻¹" in our calculations and graphs. The P retention efficiency was also calculated

with the ratio between the accumulation rate at surface sediment and burial rate at stabilized depth (Ingall and Jahnke, 1994).

3. Result

3.1. Sediment and water properties

The physicochemical properties of the water column and surface sediment are shown in Table S1. SRP in the water column ranged between 0.004 mg/L to 0.26 mg/L (averaged 0.049 mg/L) and TP concentration ranged between 0.082 mg/L to 0.742 mg/L (averaged 0.215 mg/L). Concentrations of SRP and TP in the west Lake Chaohu (averaged 0.09 mg/L and 0.29 mg/L respectively) were higher than those in the east Lake Chaohu (averaged 0.02 mg/L and 0.17 mg/L respectively), with the highest SRP and TP concentrations at site S1. Similarly, the Chl-a concentrations were higher in the west (95.6 µg/L) than that in the east (18.6 µg/L) and ranged from 2 µg/L to 290.3 µg/L (averaged 48.2 µg/L) in the whole lake; the organic matter content in surface sediment was higher in the west (1.97%) than that in the east (1.83%), ranging from 0.57% to 2.99% (averaged 1.9%) in the whole lake.

3.2. Porewater profiles of SRP, NH_4^+-N, Fe^{2+} and their fluxes

The vertical distributions of SRP in the porewaters were shown in Fig. 2 (a). Most profiles exhibited similar patterns with SRP concentrations increasing rapidly with depth until reaching a peak, followed by a gradually decreasing trend with depth, except at sites S5, S6, S8, and S12, the SRP concentrations were relatively steady with depth after reaching a peak value (Fig. 2 (a)). In the west lake except for S5, the SRP peaks appeared at around 2 cm below the SWI, with concentrations varied from 0.53 mg/L to 3.9 mg/L (averaged 2.17 mg/L). While in the east lake, the peaks appeared deeper, at around 3 cm below the SWI, and the concentrations varied between 0.84 mg/L to 1.19 mg/L (averaged 1.08 mg/L), which was half of that in the west lake.

The porewater profiles of NH_4^+ and Fe^{2+} were also shown in Figs. 2 (b) and Fig. 3 (c). Fe^{2+} concentration increased rapidly below the SWI and stayed relatively constant in the deep sediments (mostly 4 cm below SWI). The Fe^{2+} concentrations varied from 0.55 mg/L to 2.3 mg/L (averaged 1.12 mg/L) in the west and from 0.83 mg/L to 1.96 mg/L (averaged 1.41 mg/L) in the east lake. The porewater NH_4^+ gradually increased with depth below SWI at all sites, reaching values between NH_4^+- N of 3.37 mg/L to 49.08 mg/L in the sediments (average NH_4^+ porewater column concentrations of all depths measured was 13.51 mg/L and 6.89 mg/L in the west and east lake, respectively).

Table S2 summarizes the average porewater concentrations of SRP, NH_4^+-N, and Fe^{2+} at all sites and their diffusive fluxes at the SWI: SRP ranged between 0.5 mg/L to 1.65 mg/L and 0.7 mg/L to 0.99 mg/L in the west lake (averaged 1.07 mg/L) and the east lake (averaged 0.86 mg/L), respectively; the diffusive fluxes of SRP in the west lake (0.2 mg/m²·d⁻¹ to 6.69 mg/m²·d⁻¹, averaged 2.76 mg/m²·d⁻¹) were more than two times higher than those in the east lake (0.73 mg/m²·d⁻¹ to 1.76 mg/m²·d⁻¹, averaged 1.05 mg/m²·d⁻¹). The Fe^{2+} fluxes were in the range of 0.15 mg/m²·d⁻¹ and 26.3 mg/m²·d⁻¹ and were highest at S1, at which the highest Fe^{2+} concentration in pore water was also found. The average Fe^{2+} flux in the west lake (9.98 mg/m²·d⁻¹) was two times that in the east lake (4.5 mg/m²·d⁻¹). The fluxes of NH_4^+-N varied between 2.25 mg/m²·d⁻¹ and 128.1 mg/m²·d⁻¹, with an average value of 33.54 mg/m²·d⁻¹ in the west lake compared with 5.43 mg/m²·d⁻¹ in the east lake (Table S2).

3.3. Phosphorus fraction in sediment

Vertical distributions of P binding forms were shown in Fig. 3. The TP content in sediment showed the highest value in the layer within the top 10 cm (419.13 mg/kg at S9 to 1134.76 mg/kg at S3) and decreased in the deeper layer (262.62 mg/kg in S1 to 742.19 mg/kg S2) (except for
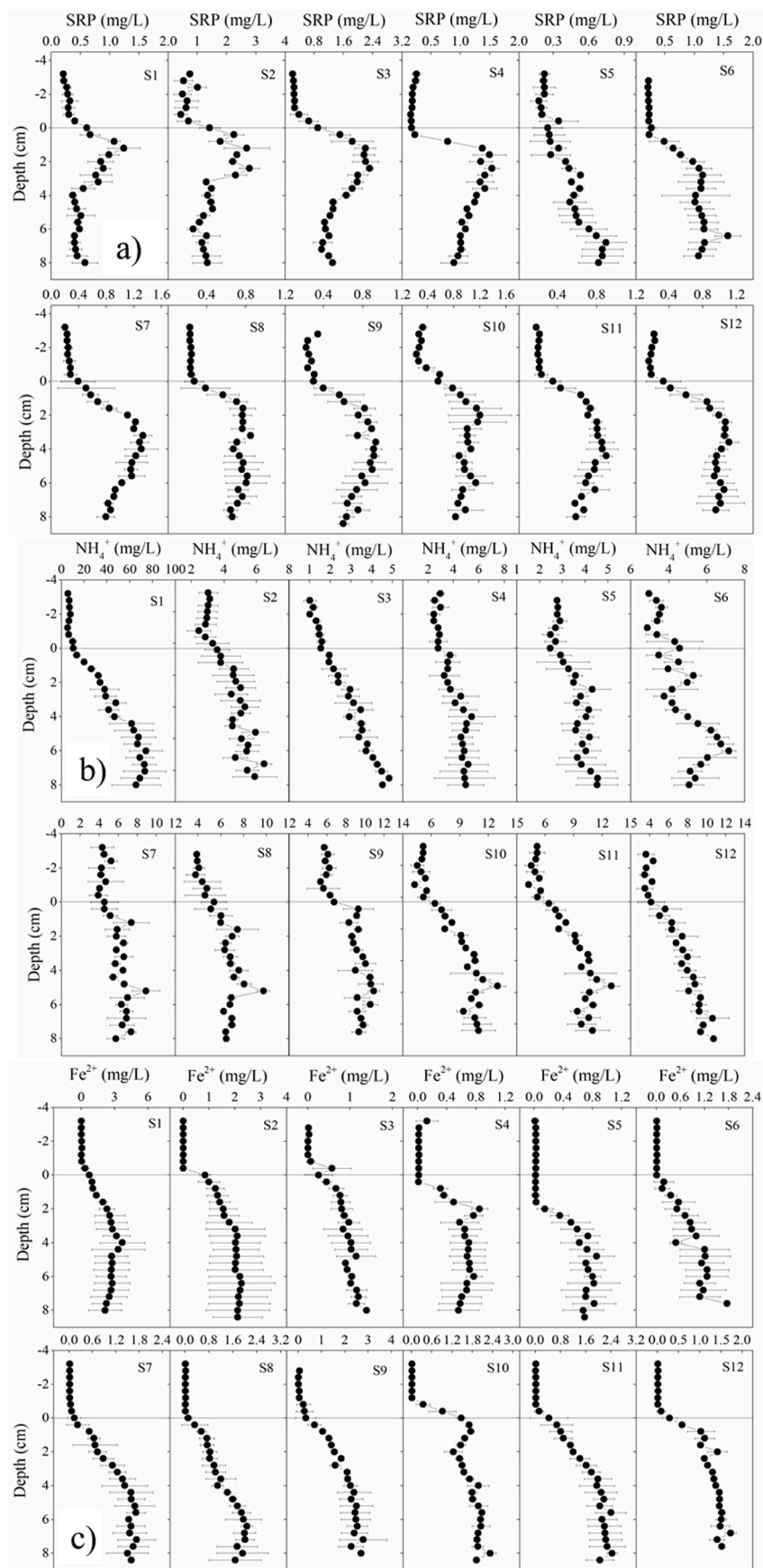
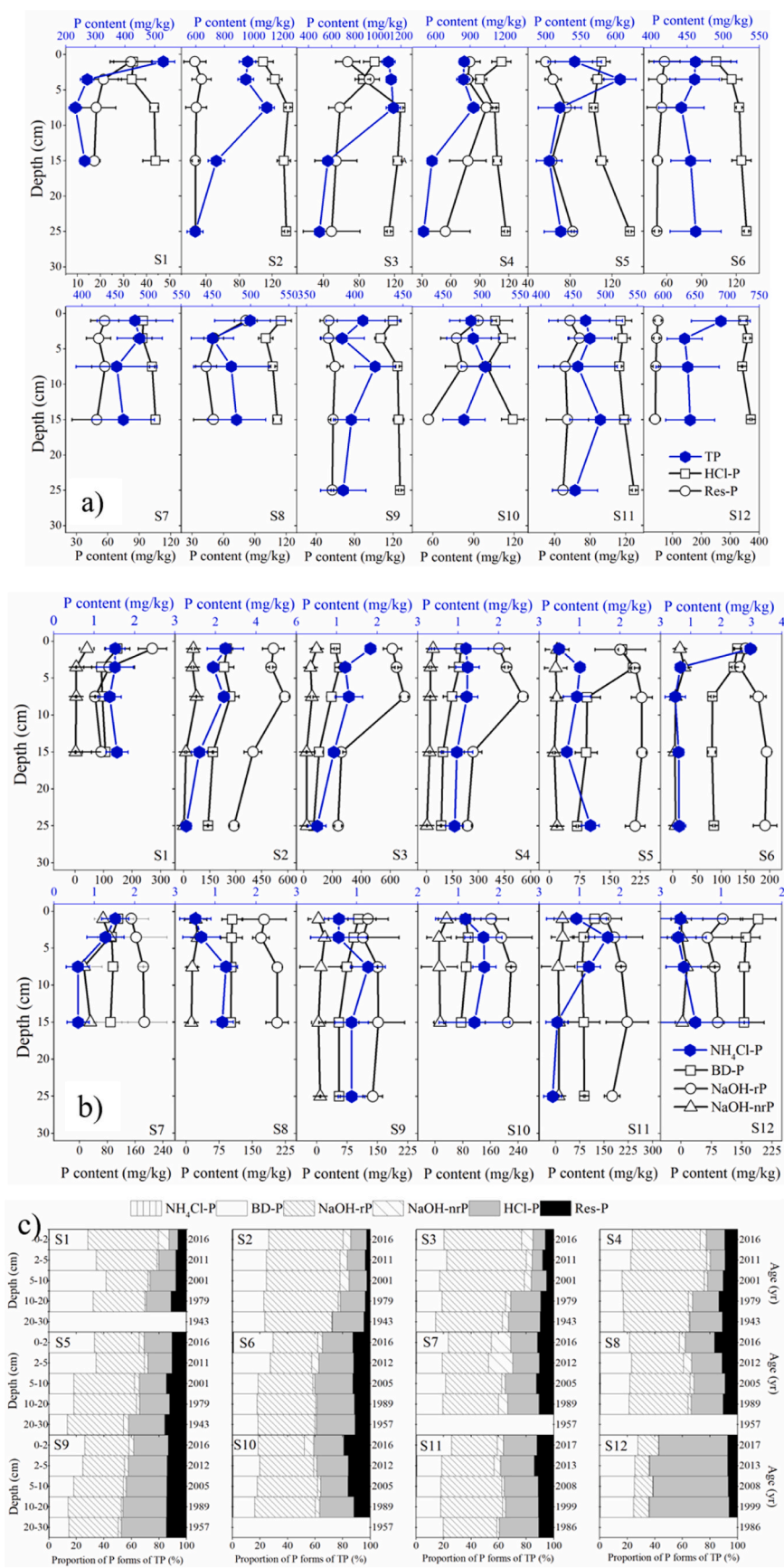**Fig. 2.** Porewater concentrations of SRP (a), NH_4^+-N (b) and Fe^{2+} (c).

Fig. 3. Vertical distribution of P binding forms (a, b) and their relative distribution (c).

S11 where there was a deeper peak at 15 cm). The concentrations of TP at most sites in the west lake (except S1) stabilized at or below 15 cm, while in the east lake, the TP content generally stabilized at 10 cm or even shallower (except S9, S10) (Fig. 3a). The aluminum-bound P (NaOH-rP) was the dominant P binding form in both surface sediment (127.08 mg/kg at S9 to 615.52 mg/kg at S3) and deep sediments (91.31 mg/kg at S1 to 289.71 mg/kg at S3) at most sites except S12 (Fig. 3b); aluminum-bound P was significantly higher than other P forms ($p <$ 0.01) (Table S3) and contributed to 32.4%–56.4% of the TP content (Fig. 3c). The relative proportion of NaOH-rP in most sites in the west lake (except S5) decreased with depth (from 49.4% to 56.4% of TP in surface sediments to 34.8%–48.6% of TP in the deep sediments (Fig. 3c). On the contrary, at most sites in the east lake (except S12), the fraction of NaOH-rP increased with depth (from 31.1% to 36.1% of TP in the surface sediment to 35.7%–44.1% of TP in the deep sediments; Fig. 3c). The redox-sensitive P (BD-P) was the second most abundant P binding form in the surface sediment (ranged from 99.09 mg/kg at S10 to 248.19 mg/kg at S2) but decreased substantially with depth and became less important in the deep sediments (ranged from 55.94 mg/kg at S9 to 156.25 mg/kg in S12; Fig. 3b), but still significantly higher than other P forms except HCl; $p <$ 0.01) (Table S3). The proportion of BD-P also decreased with depth at all sites from a higher value in the surface sediments (18.3%–28.8% of TP) to a lower value in the deepest sediments (13.3%–29.2% of TP) (Fig. 3c). Contrary to BD-P, the concentrations of carbonate-bound P (HCl–P) in the surface sediment (ranged from 34.09 mg/kg at S1 to 344.66 mg/kg at S12) was lower than BD-P, but became more important in the deep sediments (higher than BD-P; ranged from 43.87 mg/kg at S1 to 371.14 mg/kg at S12) (Fig. 3a): the percentage of HCl–P at all sites increased with depth from a lower value in the surface sediments (from 6.4% to 49.8% of TP) to a higher value in the deep sediments (from 16.7% to 57.8% of TP) (Fig. 3c). The NaOH-nrP, NH$_4$Cl–P and Res-P were the P forms that contributed least to the TP in the sediments (Three forms are significantly different from other P forms, $p <$ 0.01, NaOH-nrP appeared not significantly different from the other two forms respectively). Both P forms showed a decreasing trend from surface to deeper sediment layer: NaOH-nrP decreased from 3.14 (S12) - 89.43 (S3) mg/kg (0.5–14% of TP) in the surface sediments to 1.27 (S2) - 30.76 (S7) mg/kg (0.2–6.7% of TP) in the deep sediments; NH$_4$Cl–P decreased from 0.33 (S12) - 2.49 (S2) mg/kg (0.05–0.6%% of TP) in the surface sediments to 0.34 (S11) - 1.27 (S5) mg/kg (0.07–0.5% of TP) in the deep sediments. The residual P (Res-P) was the most stable P form and showed a relatively homogeneous vertical distribution, 26.35 mg/kg (S2) to 93.3 (S10) mg/kg (2.7%–19.2% of TP) in the surface sediments and 17.34 (S1) mg/kg to 86.81 (S10) mg/kg (4.5%–15.8% of TP) in the deepest sediments.

3.4. Long-term net phosphorus release and potentially mobile P pool

The short-term and long-term net P release rates were shown in Fig. 4. The long-term net P release ranged from 0.41 mg/m^2·d^{-1} to 8.94 mg/m^2·d^{-1} (averaged 2.98 mg/m^2·d^{-1}) and the average long-term net P release rate in the west lake (5.34 mg/m^2·d^{-1}) was 4 times higher than that in the east lake (1.3 mg/m^2·d^{-1}). In the west lake and two sites in the east lake that are close to riverine input (S11 and S12), the long-term P release rate was comparable to or even higher than the short-term P release rate, while the trends are opposite at other sites (most of the east lake except S11 and S12).

The potential mobile P pools and P fractions release rates were shown in Fig. 5. The composition of potential mobile P pools varied among sites. At most sites in the west (S1, S2, S3, S4) and S12 in the east, the potential mobile P pools consisted of NH$_4$Cl–P, BD-P, NaOH-rP and NaOH-nrP, while at the other sites (most sites in the east and S5 in the west) NaOH-rP was not mobile. The BD-P was the dominant P form at most sites in the east that contributed to P releasem, ranging from 0.08 g/m^2 to 3.35 g/m^2 (averaged 1.46 g/m^2) and released between 0.03 mg/m^2·d^{-1} to 2.23 mg/m^2·d^{-1} (averaged 0.98 mg/m^2·d^{-1}) of P in the long
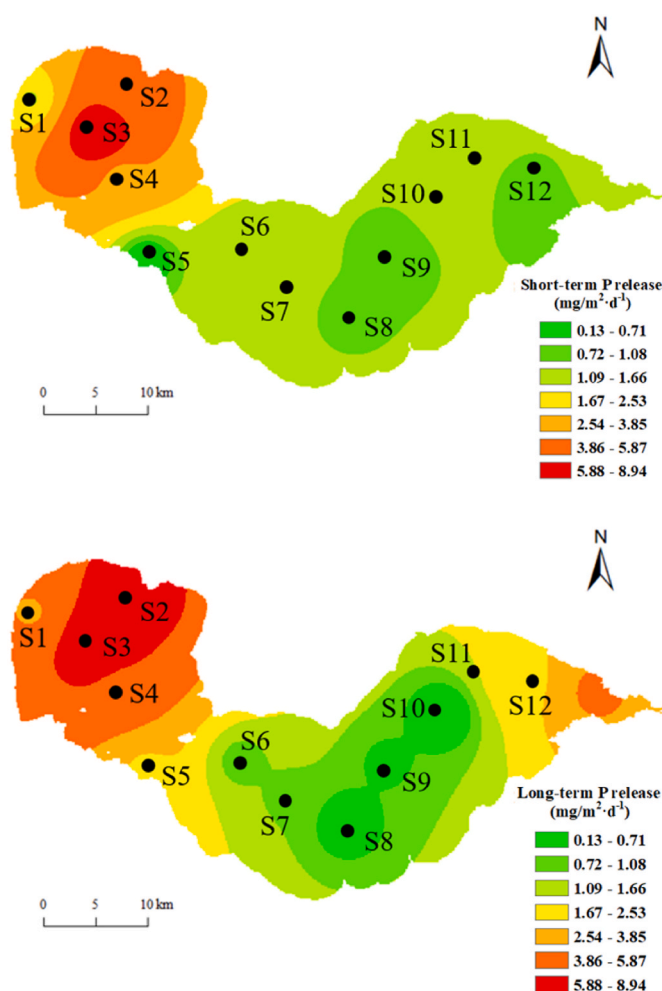

Fig. 4. Short-term (a) and long-term P (b) release in Lake Chaohu.

term. NaOH-rP contributed more at most sites in the west lake (except S5) and varied from 1.08 g/m^2 to 3.47 g/m^2 (averaged 2.45 g/m^2) and released between 2.36 mg/m^2·d^{-1} to 4.65 mg/m^2·d^{-1} (averaged 3.59 mg/m^2·d^{-1}). P immobilization due to formation of HCl–P varied from 0.03 g/m^2 to 1.84 g/m^2 (averaged 0.6 g/m^2) and its rate ranged from 0.01 mg/m^2·d^{-1} to 0.1 mg/m^2·d^{-1} (averaged 0.05 mg/m^2·d^{-1}). In the east lake, NaOH-rP, varied from 0.5 g/m^2 to 2.65 g/m^2 (averaged 1.32 g/m^2), also contributed to immobilization at some sites with rates ranging from 0.01 mg/m^2·d^{-1} to 0.36 mg/m^2·d^{-1} (averaged 0.16 mg/m^2·d^{-1}). The P retention efficiency of TP varied between 16% and 96%, with a higher average value of 80% in the east lake than the average of 36% in the west lake (Table 1).

4. Discussion

4.1. Short-term phosphorus fluxes contributed by organic P degradation and release of legacy P

Short-term phosphorus release reflects the transient P recycled from sediment to water column and is strongly sensitive to the dynamics of oxygen, redox conditions, pH, temperature, bioturbation and hydrodynamic conditions (Hupfer and Lewandowski, 2008; Jensen and Andersen, 1992; Reed et al., 2011). The calculated diffusive fluxes in the summer might underestimate the real release rate if other processes are important (such as hydrodynamic disturbance, sediment resuspension (Yang et al., 2020) and bioturbation), but they provide useful insights for understanding short-term P release rates and have been used to
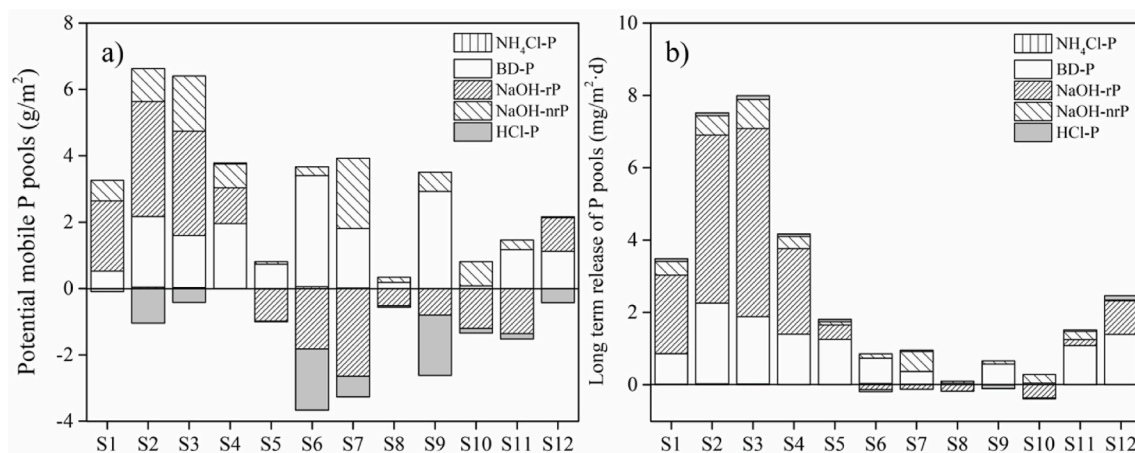
Fig. 5. Potentially mobile P Pools (a) (negative numbers represent immobilization and burial) and their release rates (b).

Table 1
P accumulation and retention and long term release.

Sampling sites	P accumulation (g/m^2·y^{-1})	P burial (g/m^2·y^{-1})	Retention total P (%)	Long term P release (g/m^2·y^{-1})
S1	1.88 ± 0.28	0.53 ± 0.08	28 ± 8	1.35 ± 0.34
S2	3.41 ± 0.67	0.78 ± 0.13	23 ± 10	2.63 ± 0.86
S3	3.88 ± 0.97	0.62 ± 0.15	16 ± 9	3.26 ± 1.02
S4	3.52 ± 0.38	1.85 ± 0.08	53 ± 7	1.67 ± 0.48
S5	1.93 ± 0.21	1.11 ± 0.14	58 ± 13	0.82 ± 0.28
S6	1.92 ± 0.09	1.63 ± 0.07	85 ± 8	0.29 ± 0.06
S7	1.99 ± 0.08	1.65 ± 0.04	83 ± 5	0.35 ± 0.06
S8	2.03 ± 0.07	1.92 ± 0.02	95 ± 4	0.11 ± 0.01
S9	1.66 ± 0.11	1.44 ± 0.08	87 ± 8	0.21 ± 0.04
S10	2.06 ± 0.05	2.01 ± 0.02	96 ± 3	0.05 ± 0.01
S11	0.43 ± 0.08	0.2 ± 0.02	47 ± 12	0.34 ± 0.07
S12	4.84 ± 0.57	3.33 ± 0.17	69 ± 13	1.51 ± 0.47

represent seasonal P release in many studies (Alam et al., 2020; Markovic et al., 2019; Yang et al., 2020). The P diffusive fluxes in Lake Chaohu in 2019 summer (0.2 mg/m^2·d^{-1} to 6.69 mg/m^2·d^{-1}, averaged 2.09 mg/m^2·d^{-1}) are relatively high compared with other eutrophic systems around the world (Table S4; Di et al., 2015; Matisoff et al., 2016; Li et al., 2008; Kowalczewska-Madura et al., 2015; Stefan Markovic et al., 2019; Beutel and Horne, 2018; Alam et al., 2020; Miao et al., 2006). Our results of P flux averaging 3.54 mg/m^2·d^{-1} in the west in summer 2019 (3.3 times higher than the P flux of 1.05 mg/m^2·d^{-1} in the east) are consistent with estimates previously in the same area using similar methods, 2.55 mg/m^2·d^{-1} in summer 2018 and 3.34 mg/m^2·d^{-1} in autumn 2018 (Yang et al., 2020). On the other hand, the fluxes estimated at one of the most polluted areas in the west lake (S2, 4 mg/m^2·d^{-1}) showed certain recovery from eutrophic (average flux of 5.28 mg/m^2·d^{-1} was estimated in March 2011 and 5.32 mg/m^2·d^{-1} was estimated in August 2013 around the same area of S2) (Liu et al., 2014; Li et al., 2015), although the site is still suffering from heavy eutrophication. This might suggest that decades of lake restoration (such as the control of nonpoint pollution and point pollution and ecological rehabilitation projects around the lake) might have help to some extend. The

timescale of lake recovery is controlled by the balance between P sedimentation and sediment P recycling (P internal loading) (Katsev, 2017). Therefore, the estimate of sediment P release on both short- and long-terms and their temporal trends is key to the development of mass balance models that can predict P dynamics in water column and guide management practices (Li et al., 2021).

Degradation of organic matter and desorption of P from ferric oxides or hydroxides are often the main processes that drive the summer short-term P release from sediment (Dittrich et al., 2013; Markovic et al., 2019; Tammeorg et al., 2015). High rates of mineralization of organic matter typically occur following phytoplankton blooms in summer, leading to high rates of organic matter degradation in the surface sediments and consequently high rates of sediment SRP release and high fluxes across the SWI (Fig. 2 and Table S2). This was also indicated by the high NH_4^+ fluxes across the SWI that came from the degradation of organic matter. Redox-sensitive ron-associated P fractions in sediments are also important sources of dissolved P: Iron (hydro)oxides can sorb dissolved P under oxic conditions and release P back to dissolved forms in anaerobic sediments (Malmaeus et al., 2012). Our results showed a simultaneous increase of SRP and Fe^{2+} concentration in the pore water (Fig. 2), and a decrease of iron-bound P (BD-P) with depth (reduce environment in deeper sediment) (Fig. 3), suggesting that P may be partially released from the reduction of iron oxyhydroxides.

To determine the contributions of organic P and iron-bound P to short-term P fluxes at the SWI, we can look at the N:P stoichiometry of the fluxes (Table S5). The ratio of NH_4^+ and SRP release from organic matter degradation should be similar to the organic N:P ratio in sediment if we can assume that nitrification, sorption of NH_4^+ can be considered negligible. Our P flux: N flux ratio averaged 0.139 (mole: mole ratio; Table S5), which was considerably larger than the sediment organic P: N ratio (Table S5, P: N = 0.01 on average) and the Redfield ratio (P:N = 0.0625). This indicates that, in Lake Chaohu, in addition to the release of P from the degradation of organic matter, dissolved P also comes from the mobilization of the legacy P (Yang et al., 2020). Based on the organic P:N ratio of 0.01 and an average NH_4^+ flux of 1.22 mmol/m^2/d (17.14 mg/m^2·d^{-1}), we can estimate, in the short-term, that 0.01 mmol/m^2/d of SRP (0.34 mg/m^2·d^{-1}) would release from the degradation of organic matter, which only accounts for 19% of the total P fluxes (Table S2), with the rest 81% of P fluxes contributed by the release of other forms such as iron-bound P that likely has been stored in the sediments as legacy P.

4.2. Long-term legacy P release compromised lake management

The long-term P release rates at sites S6– S9 (in the open waters of the east lake) were lower than the short-term P release rates measured in

the summer. In other seasons, organic P deposition and P mobilization can be lower than those in the summer, leading to lower P fluxes over the long term compared to summer transient P release. More data is needed to understand whether the high P flux we measured represents a typical summer transient flux that is higher than long-term P fluxes. Nevertheless, our data suggested that to estimate the short-term P fluxes and P retention and release, one may not rely on a transient value at the time of measurement.

At sampling sites in the west lake and near the river outputs of the east end (S11 and S12), the P release rates were much higher, and the long-term P release rates appeared similar or higher than the short-term P release rates (Fig. 4). This indicates that high internal P loading has occurred for years and even decades. i.e., 29 years for most areas of the west lake (an average sedimentation rate of 9.8 mg/m$^2 \cdot$d^{-1} and a depth of 15 cm) and 6 years for sites S11 and S12 (an average sedimentation rate of 14.32 mg/m$^2 \cdot$d^{-1} and a depth of 5 cm), although seasonality might still exist (Yang et al., 2020). This explains the long-lasting algae bloom in west lake Chaohu for nearly a decade even after the reduction of external P inputs (Yang et al., 2020). Notably, long-term P release at S11 and S12 were higher compared with the other sites in the east lake, likely due to the shallower water depth (about 1.5m) resulting in higher P sedimentation (settled debris) as the algal debris take less time to settle and decay before reaching sediments, as well as their proximity to the river inlets. There, the fact that short-term release (in summer) is marginally lower than the long-term release, which may suggest that the lake had been suffering from severe eutrophication in the past but is now in the process of slowly recovering. This is likely due to the increasingly high standard for controlling external P input and the ecological remediation in the basin. Nevertheless, the high long-term P release rate suggests that sediment can serve as a long-term P source into the water column, compromising lake management efforts.

4.3. P release and retention mechanisms

The vertical distributions of P binding pools reflect the P release mechanism and diagenetic transformations processes (Fig. 3). For the whole lake, the long-term release potential of iron bond P (BD-P) (averaged 0.87 mg/m$^2 \cdot$d^{-1}) contributed most to the long term release rate (averaged 52.1%) (Fig. 5; calculated by the difference between P fraction accumulation at the sediment surface and P fraction buried at its stabilization depth). Similarly, the degradation of organic P form (NaOH-nrP, averaged 0.25 mg/m$^2 \cdot$d^{-1}; decreased with depth and mostly stabilized at the same depth with BD-P) in the surface sediment also substantially contributed (averaged 34.3%). The long-term release potential of BD-P and NaOH-nrP were both higher in the west (averaged 1 mg/m$^2 \cdot$d^{-1} and 0.27 mg/m$^2 \cdot$d^{-1} respectively) than that in the east (averaged 0.59 mg/m$^2 \cdot$d^{-1} and 0.18 mg/m$^2 \cdot$d^{-1} respectively). This is likely because of the persistent external pollution from the inflowing rivers into the west lake increasing organic P sedimentation and consequently the accumulation of sediment legacy P.

Interestingly, the pool of Al hydroxides bond P (NaOH-rP) in the two regions exhibited contrary trends: NaOH-rP contributed to long-term P burial at most sites in the east lake while contributed to long-term release at most sites in the west lake (Fig. 5). The NaOH-rP is conventionally regarded as a stable P sink (permanently buried), which is insensitive to changes in redox conditions (Alam et al., 2020; Kopacek et al., 2005). In the east lake, it contributed about 1%–36% to the total burial (Fig. 5). However, several studies also highlighted the complex nature of this binding pool (Lukkari et al., 2007; Markovic et al., 2019; Yang et al., 2020) and suggested that may be partly reactive and contribute to sediment P release. The studies showed that at pH > 8 or when porewater Si concentrations were high, ligand exchange reactions in Al hydroxides could induce dissolution of P (Golterman, 1977; Koski-Vähälä et al., 2001; Lijklema, 1980). This is consistent with the high pH in the sediments in the west lake and the appeared long-term release of NaOH-rP (Table S1). The calcium-bound P (HCl–P) is

thought to contribute to permanent P retention, which increased with depth at all sampling sites (for both HCl–P and the ratio of HCl–P: TP) (Fig. 3c), accounting for 16.7%–57.8% of the TP in the deep sediments. This indicates that liable P forms have switched to stable HCl–P form contributing to P burial (average 23% of the potential mobilized P pools), as the change of watershed HCl–P input influencing its vertical distribution in sediments is unlikely: the dramatic changes of land use (decrease of farm land and increase of construction land) in Chaohu watershed occurred after 2000 (Huang et al., 2015), corresponding to the sediment depth of <10 cm based on sediment dating, while no obvious increase of HCl–P/TP input were likely to happen.

4.4. Implications for lake-wide P budget and lake eutrophication

Using the average long-term P release rates in both the east and west and the area of Lake Chaohu (250 km^2 and 518 km^2 for the west lake and east lake respectively), we estimate the total sediment long-term P release from Lake Chaohu as 698 t P/year. The long-term sediment P release in Lake Chaohu contributed as much as 69% of the external P inputs (average annual P inputs of Lake Chaohu from 2014 to 2018 was 1011 t P/year) (Wang et al., 2020), of which the west lake (33% area of the whole lake) contributed disproportionally, to 70% of the overall sediment P release. The long-term P release offset the outputs of 526 t P/year via outflow and exceeded the magnitude of the hydrodynamic P retention (input – output = 485 t P/year).

The high magnitude of long-term P release and the low retention efficiency of the west lake (average 36%) (Table S3) implicated that high organic P deposition in shallow eutrophic lakes can lead to accumulation of legacy P in sediment that can be released over the long term, contributing to internal P loading (Markovic et al., 2019). Therefore, in addition to the increasingly stricter limit of P external loading to control lake eutrophications, we need to consider preventing internal P release from sediments, particularly from legacy P. We propose exploring various approaches, including large-scale sediment dredging while avoiding sediment resuspension and re-settlement that may offset the efforts (Liu et al., 2000; Zhong et al., 2021). As wind-induced sediment resuspension might frequently occur in shallow lakes and increase P fluxes, especially in sediments with high legacy P and dissolved P concentrations similar to those in Lake Chaohu, we also proposed applying in-situ capping methods along the heavily polluted lakeshore.

5. Conclusion

Our study showed that, in Lake Chaohu, sediment internal P loading was an important source of P in the water column, and the west lake contributed disproportionally to both short-term and long-term P releases. In the east lake, the summer P release was higher than the long-term P release, therefore this snapshot measurement would overestimate sediment P release if taken as an average. On the contrary, in the west lake, short-term summer P release now is comparable or even lower than the long-term P release, indicating that water quality might be slowly recovering in this most severely eutrophic region of the lake after decades of management efforts, although the long-term release of legacy P, partially via degradation of organic matter and more importantly reductive dissolution of iron-bound P, has likely impeded the water quality recovery over years or even decades. Notably, while the sediment Al oxides can adsorb P and increase P retention in the sediments in the east lake, P can be partly desorbed from Al-bound P that acts as a long-term P source at most sites in the west lake, possibly due to the high alkaline pore water and elevated Si concentrations. Our study quantified the internal P loading in whole Lake Chaohu and demonstrated that we can combine short-term and long-term studies of P release to help understand P cycling in eutrophic lakes and guide lake water quality management.

Declaration of competing interest

The authors declare that they have no known competing financial interests or personal relationships that could have appeared to influence the work reported in this paper.

Appendix A. Supplementary data

Supplementary data to this article can be found online at https://doi.org/10.1016/j.envpol.2021.118471.

Credit author contribution statement

Chunhui Yang: Data curation, Writing - original draft, Software, Investigation. **Jiying Li:** Formal analysis, Writing - review & editing, Methodology. **Hongbin Yin:** Conceptualization, Methodology, Supervision.

References

Alam, M.S., Barthod, B., Li, J., Liu, H., Zastepa, A., Liu, X., Dittrich, M., 2020. Geochemical controls on internal phosphorus loading in Lake of the Woods. Chem. Geol. 558, 119873.

Beutel, M.W., Horne, A.J., 2018. Nutrient Fluxes From Profundal Sediment of Ultra-Oligotrophic Lake Tahoe, California/Nevada: Implications for Water Quality and Management in a Changing Climate. Water Resour. Res. 54, 1549–1559.

Carey, C.C., Rydin, E., 2011. Lake trophic status can be determined by the depth distribution of sediment phosphorus. Limnol. Oceanogr. 56, 2051–2063.

Chinese EPA, 2002. Methods for the Examination of Water and Wastewater, Fourthed. China Environmental Science Press, Beijing.

Depew, D.C., Koehler, G., Hiriart-Baer, V., 2018. Phosphorus dynamics and availability in the nearshore of eastern lake erie: insights from oxygen isotope ratios of phosphate. Front. Mar. Sci. 5, 215.

Di, Z., Zhang, H., Shan, B., 2015. Status of internal nutrient loads and their effects on overlying water quality in Taihu Lake. J. Environ. Sci. 35 (12), 3872–3882.

Ding, S.M., Chen, M.S., Gong, M.D., Fan, X.F., Qin, B.Q., Xu, H., Gao, S.S., Jin, Z.F., Tsang, D.C.W., Zhang, C.S., 2018. Internal phosphorus loading from sediments causes seasonal nitrogen limitation for harmful algal blooms. Sci. Total Environ. 625, 872–884.

Dittrich, M., Chesnyuk, A., Gudimo, A., McCulloch, J., Quazi, S., Young, J., Winter, J., Stainsby, E., Arhonditsis, G., 2013. Phosphorus retention in a mesotrophic lake under transient loading conditions: insights from a sediment phosphorus binding form study. Water Res. 47, 1433–1447.

Golterman, H., 1977. The role of iron in the exchange of phosphate between water and sediments. Interact. Sediments Fresh Water 286–293.

Huang, M.Y, He, X., Wu, D., Wu, Y., Wang, S.C., 2015. Study of Land Use Degree Change and Its Spatial Heterogeneity in Chaohu Lake Basin. Soils 47 (5), 994–1000.

Hupfer, M., Lewandowski, J., 2005. Retention and early diagenetic transformation of phosphorus in Lake Arendsee (Germany) - consequences for management strategies. Arch. Hydrobiol. 164, 143–167.

Hupfer, M., Lewandowski, J., 2008. Oxygen controls the phosphorus release from Lake sediments – a long-lasting paradigm in Limnology. Int. Rev. Hydrobiol. 93, 415–432.

Ingall, E., Jahnke, R., 1994. Evidence for enhanced phosphorus regeneration from marine-sediments overlain by oxygen depleted waters. Geochem. Cosmochim. Acta 58, 2571–2575.

Jensen, H.S., Andersen, F.O., 1992. Importance of temperature, nitrate, and ph for phosphate release from aerobic sediments of 4 shallow, eutrophic lakes. Limnol. Oceanogr. 37, 577–589.

Katsev, S., 2017. When large lakes respond fast: a parsimonious model for phosphorus dynamics. J. Great Lake. Res. 43, 199–204.

Katsev, S., Tsandev, I., L'Heureux, I., Rancourt, D.G., 2006. Factors controlling long-term phosphorus efflux from lake sediments: exploratory reactive-transport modeling. Chem. Geol. 234, 127–147.

Kim, D.K., Zhang, W.T., Rao, Y.R., Watson, S., Mugalingam, S., Labencki, T., Dittrich, M., Morley, A., Arhonditsis, G.B., 2013. Improving the representation of internal nutrient recycling with phosphorus mass balance models: a case study in the Bay of Quinte, Ontario, Canada. Ecol. Model. 256, 53–68.

Kopacek, J., Borovec, J., Hejzlar, J., Ulrich, K.U., Norton, S.A., Amirbahman, A., 2005. Aluminum control of phosphorus sorption by lake sediments. Environ. Sci. Technol. 39, 8784–8789.

Koski-Vähälä, J., Hartikainen, H., Tallberg, P., 2001. Phosphorus mobilization from various sediment pools in response to increased pH and silicate concentration. J. Environ. Qual. 30, 546–552.

Li, C., Tan, Z., Liu, Z., Wang, J., Zhu, G., Zhang, X., 2008. Nutrient release in the sediments of Huizhou West Lake. Ecol. Environ. 17, 537–541.

Li, C., Wang, D., Yang, J.Y., Wang, Y., Ding, S.M., 2015. In situ high-resolution analysis of labile phosphorus in sediments of Lake Chaohu. Environ. Sci. 36 (6), 2077–2084.

Kowalczewska-Madura, K., Gołdyn, R., Dera, M., 2015. Spatial and seasonal changes of phosphorus internal loading in two lakes with different trophy. Ecol. Eng. 74, 187–195.

Li, J., Ianaiev, V., Huff, A., Zalusky, J., Ozersky, T., Katsev, S., 2021. Benthic invaders control the phosphorus cycle in the world's largest freshwater ecosystem. Proc. Natl. Acad. Sci. Unit. States Am. 118, e2008223118.

Lijklema, L., 1980. Interaction of orthophosphate with iron(III) and aluminum hydroxides. Environ. Sci. Technol. 14, 537–541.

Liu, C., Shao, S., Shen, Q., Fan, C., Zhang, L., 2000. Effects of riverine suspended particulate matter on the post-dredging increase in internal phosphorus loading across the sediment-water interface. Environ. Pollut. 144, 2329–2335.

Liu, C., Shao, S.G., Fan, C.X., Zhou, Q.L., Shen, Q.S., 2014. Distribution and release risk of nutrients in the sediments of heavily polluted confluence bay of Chaohu lake. Res. Environ. Sci. 27, 1258–1264.

Lukkari, K., Hartikainen, H., Leivuori, M., 2007. Fractionation of sediment phosphorus revisited. I: fractionation steps and their biogeochemical basis. Limnol Oceanogr. Methods 5, 433–444.

Malmaeus, J.M., Rydin, E., Jonsson, P., Lindgren, D., Karlsson, O.M., 2012. Estimating the amount of mobile phosphorus in Baltic coastal soft sediments of central Sweden. Boreal Environ. Res. 17, 425–436.

Markovic, S., Liang, A.Q., Watson, S.B., Guo, J., Mugalingam, S., Arhonditsis, G., Morley, A., Dittrich, M., 2019. Biogeochemical mechanisms controlling phosphorus diagenesis and internal loading in a remediated hard water eutrophic embayment. Chem. Geol. 514, 122–137.

Matisoff, G., Carson, M.L., 2014. Sediment resuspension in the lake erie nearshore. J. Great Lake. Res. 40, 532–540.

Matisoff, G., et al., 2016. Internal loading of phosphorus in western Lake Erie. J. Great Lake. Res. 42, 775–788.

Miao, S.Y., Delaune, R.D., Jugsujinda, A., 2006. Sediment nutrient flux in a coastal lake impacted by diverted Mississippi River water. Chem. Ecol. 22, 437–449.

Murphy, J., Riley, J.P., 1962. A modified single solution method for the determination of phosphate in natural waters. Anal. Chim. Acta 27, 31–36.

Ozersky, T., Barton, D.R., Hecky, R.E., Guildford, S.J., 2013. Dreissenid mussels enhance nutrient efflux, periphyton quantity and production in the shallow littoral zone of a large lake. Biol. Invasions 15, 2799–2810.

Parsons, C.T., Rezanezhad, F., amp, apos, Connell, D.W., Van Cappellen, P., 2017. Sediment phosphorus speciation and mobility under dynamic redox conditions. Biogeosci. Discuss. 14, 1–36.

Puttonen, I., Mattila, J., Jonsson, P., Karlsson, O.M., Kohonen, T., Kotilainen, A., Lukkari, K., Malmaeus, J.M., Rydin, E., 2014. Distribution and estimated release of sediment phosphorus in the northern Baltic Sea archipelagos. Estuarine. Coastal Shelf Sci 145, 9–21.

Qian, B., Liu, L., Xiao, X., 2011. Comparative tests on different methods for content of soil organic matter[J]. J. Hohai Univ. (Nat. Sci.) 39 (1), 34–38.

Reed, D.C., Slomp, C.P., Gustafsson, B.G., 2011. Sedimentary phosphorus dynamics and the evolution of bottom-water hypoxia: a coupled benthic-pelagic model of a coastal system. Limnol. Oceanogr. 56, 1075–1092.

Ribeiro, D.C., Martins, G., Nogueira, R., Cruz, J.V., Brito, A.G., 2008. Phosphorus fractionation in volcanic lake sediments (Azores, Portugal). Chemosphere 70, 1256–1263.

Ritchie, R.J., 2006. Consistent sets of spectrophotometric chlorophyll equations for acetone, methanol and ethanol solvents. Photosynth. Res. 89, 27–41.

Rydin, E., 2000. Potentially mobile phosphorus in Lake Erken sediment. Water Res. 34, 2037–2042.

Rydin, E., Malmaeus, J.M., Karlsson, O.M., Jonsson, P., 2011. Phosphorus release from coastal Baltic Sea sediments as estimated from sediment profiles. Estuarine. Coastal Shelf Sci 92, 111–117.

Schindler, D.W., Carpenter, S.R., Chapra, S.C., Hecky, R.E., Orihel, D.M., 2016. Reducing phosphorus to curb lake eutrophication is a success. Environ. Sci. Technol. 50, 8923–8929.

Sondergaard, M., Jensen, J.P., Jeppesen, E., 2003. Role of sediment and internal loading of phosphorus in shallow lakes. Hydrobiologia 506, 135–145.

Tammeorg, O., Horppila, J., Laugaste, R., Haldna, M., Niemistö, J., 2015. Importance of diffusion and resuspension for phosphorus cycling during the growing season in large, shallow Lake Peipsi. Hydrobiologia 760, 133–144.

Tu, Q.Y., Gu, D.X., Yin, C.Q., Xu, Z.R., Han, J.Z., 1990. The Chao Lake—study on eutrophication. University of Science and Technology of China Press, Hefei.

Wang, Y.P., Kong, X.Z., Peng, Z.L., Zhang, H., Liu, G., Hu, W.P., Zhou, X.Q., 2020. Retention of nitrogen and phosphorus in Lake Chaohu, China: implications for eutrophication management. Environ. Sci. Pollut. Res. 27, 41488–41502.

Yang, C., Yang, P., Geng, J., Yin, H., Chen, K., 2020. Sediment internal nutrient loading in the most polluted area of a shallow eutrophic lake (Lake Chaohu, China) and its contribution to lake eutrophication. Environ. Pollut. 262, 114292.

Zan, F., Huo, S., Xi, B., Li, Q., Liao, H., Zhang, J., 2011. Phosphorus distribution in the sediments of a shallow eutrophic lake, Lake Chaohu, China. Environ. Earth Sci. 62, 1643–1653.

Zhang, L., Fan, C.X., Wang, J.J., Zheng, C.H., 2006. Space-time dependent variances of ammonia and phosphorus flux on sediment-water interface in Lake Taihu. Environ. Sci. 27, 1537–1543.

Zhong, J., Wen, S., Zhang, L., Wang, J., Liu, C., Yu, J., Zhang, L., Fan, C., 2021. Nitrogen budget at sediment–water interface altered by sediment dredging and settling particles: benefits and drawbacks in managing eutrophication. J. Hazard Mater. 406, 124691.